

Supplementary Information

CO adsorption on amorphous silica-alumina: electrostatic or Brønsted acidity probe ?

Fabien Leydier,^{a,b} Céline Chizallet,^{*a} Dominique Costa^b and Pascal Raybaud^a

^a *IFP Energies nouvelles, Rond-point de l'échangeur de Solaize, BP3, 69360 Solaize, France*

^b *Laboratoire de Physico-Chimie des Surfaces, CNRS-ENSCP (UMR 7045), École Nationale Supérieure de Chimie de Paris, 11 rue Pierre et Marie Curie, 75005 Paris, France*

S1.Computational methods	2
S2.Systems under study.....	3
S3. Adsorption energies, frequency shifts and Bader charges	4
S4.Lutidine / CO graphical comparison	5
References	6

S1. Computational methods

The periodic calculations were performed using density functional theory (DFT) within the Perdew and Wang PW91^[1] generalized gradient approximation and projected augmented wave (PAW) pseudo-potentials^[2] as implemented in the VASP 4.6 code^[3, 4]. The energy cut-off was set to 500 eV and forces on relaxed atoms were chosen inferior to 2×10^{-2} eV Å⁻¹ to ensure convergence accuracy.

Adsorption energies $\Delta_{\text{ads}}U$ of CO were defined according to Eq. (1) ($U_{\text{surf-CO}}$, U_{surf} , and U_{CO} are the energies of the surface with and without CO and of the CO molecule, respectively). Dipolar corrections are included in the energy calculations to take into account the effect of non-symmetrical surfaces in periodic cells.

$$\Delta_{\text{ads}}U = U_{\text{surf-CO}} - U_{\text{surf}} - U_{\text{CO}} \quad (1)$$

The harmonic C≡O stretching frequencies were calculated with an optimal displacement of ± 0.02 Å around the equilibrium atomic positions. Atoms close to the probed surface sites were also allowed to vibrate for better accuracy (typically the probed OH-group, the Si or Al atom attached to it, and second neighbors oxygen atoms). The anharmonicity corrections were calculated by exploring manually the potential energy surface along one direction – the axis determined by the C and the O atoms –, at constant position of the center of mass of the C≡O vibrator, in the range $[-0.3; +0.4]$ Å around the equilibrium C≡O bond length. For the gas phase molecule as for the CO adsorbed on each ASA site, these anharmonic corrections were all equal to -27 cm⁻¹, hence we report in the following harmonic $\tilde{\nu}_{\text{CO}}$ shifts – difference between the CO stretching frequencies of the molecule adsorbed and the one of the gas phase molecule.

Atomic charges were calculated using Bader charge analysis^[5, 6]. Electronic clouds evolutions ΔEC were obtained from difference of electronic densities (see in the text for more details, all the systems calculated have the same integration grid parameters). The visualizations of ΔEC were done using the VESTA code^[7]. The local electrostatic potential was calculated directly with VASP by generating LOCPOT files and data were extracted with VESTA.

S2. Systems under study

The reference systems for ASA^[8, 9], γ -Al₂O₃^[10, 11], amorphous silica^[12] and model mordenite are the same systems used in our previous lutidine adsorption study^[13]. For planar surfaces, the vacuum between model slabs is kept the same as the one used for lutidine adsorption in order to avoid interactions between slabs. Brønsted acid sites on the ASA surface are labeled in Fig. S1. Note that we only used the surface model exhibiting $\theta_{\text{OH}} = 5.4 \text{ nm}^{-2}$ because the bridging site included in the $\theta_{\text{OH}} = 6.4 \text{ nm}^{-2}$ model is not accessible for the CO adsorption since it is parallel to the surface and about 2 Å under the mean OH-groups plane, leading to the desorption of the CO molecule away from this site.

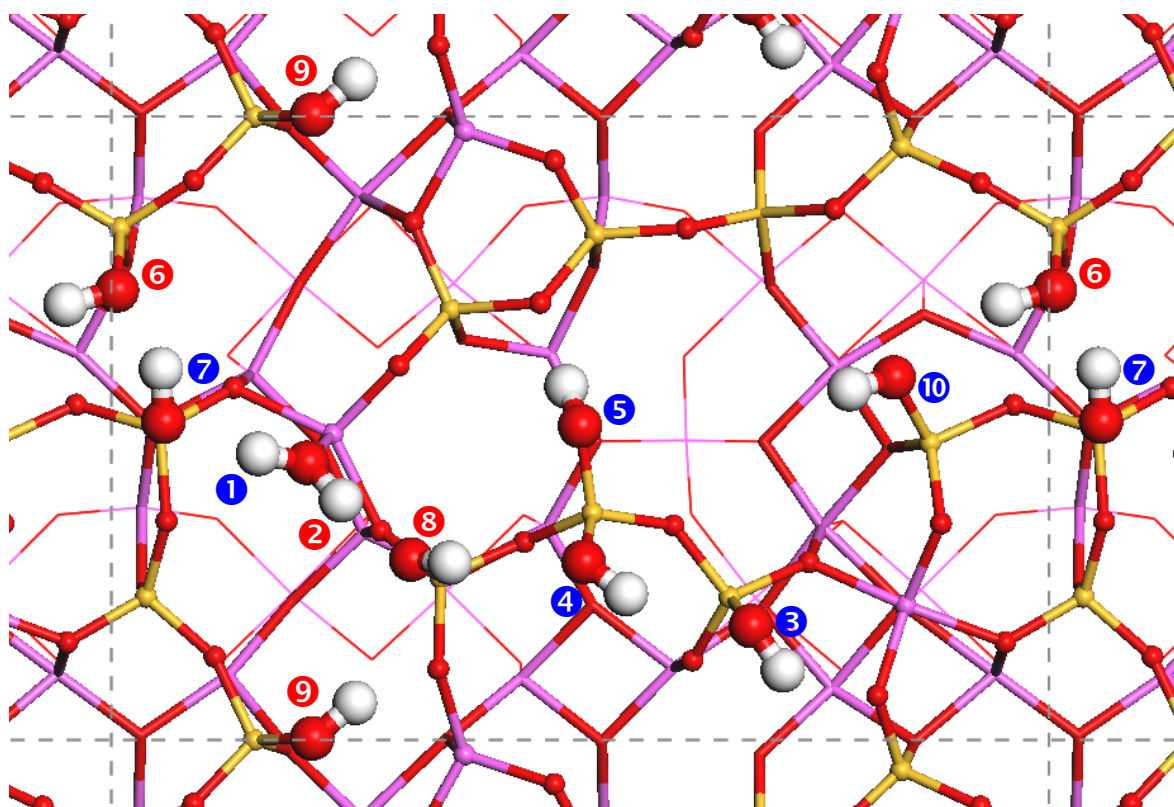


Fig. S1. ASA surface model (top view), site labels used in the main text and figures. Red labels show the sites able to proton transfer to lutidine. (Table S1 in S3 gives the description of each site according to our previous publication)^[13]

S3. Adsorption energies, frequency shifts and Bader charges

Table S1. Adsorption energy of CO and lutidine, and IR frequency of the probes. Reference calculations on amorphous silica, γ -alumina and mordenite are also provided. Red labels and frequencies show the sites able to proton transfer to lutidine.

Material	Type of site	Localization ^[13]	Label	CO E_{ads}	$\Delta\nu_{\text{CO}}$	$\Delta\nu_{\text{CO exp}}$	ν_{8a} lutidine
ASA	PBS - Si	Si(U ₁)-OH ... Si(V ₂)	6	-7	17	35, 31, 14 ^[14]	1615
	Potential PBS - Al	Si(V ₁)-OH...Al _{IV}	9	+6	34		1614
		Si(Z ₂)-OH...Al _V	10	-22	37		1596
		Si(Y ₂)-OH...Al _V	3	-10	9		1586
		Si(X ₂)-OH ₍₁₎ ...Al _{IV}	5	+7	23		1587
	Silanol-Al	Si(W ₂)-OH Si(V ₂)-OH	8 7	-19 -9	24 20		1613 1593
Si-OH	Si(X ₂)-OH ₍₂₎	4	-13	15	1590		
Al-OH	Al-HOH ₍₁₎	1	-4	24	1592		
	Al-HOH ₍₂₎	2	-2	6	1605		
Silica	Isolated silanol			-15	26	16 ^[15]	1591
	Hydrogen nest			-23	41		1599
γ -alumina	(110) III-12			-16	13	10 ^[16]	1585
mordenite	Bridging hydroxyl Si-(OH)-Al			-30	54	35 ^[14] , 36 ^[17]	1616

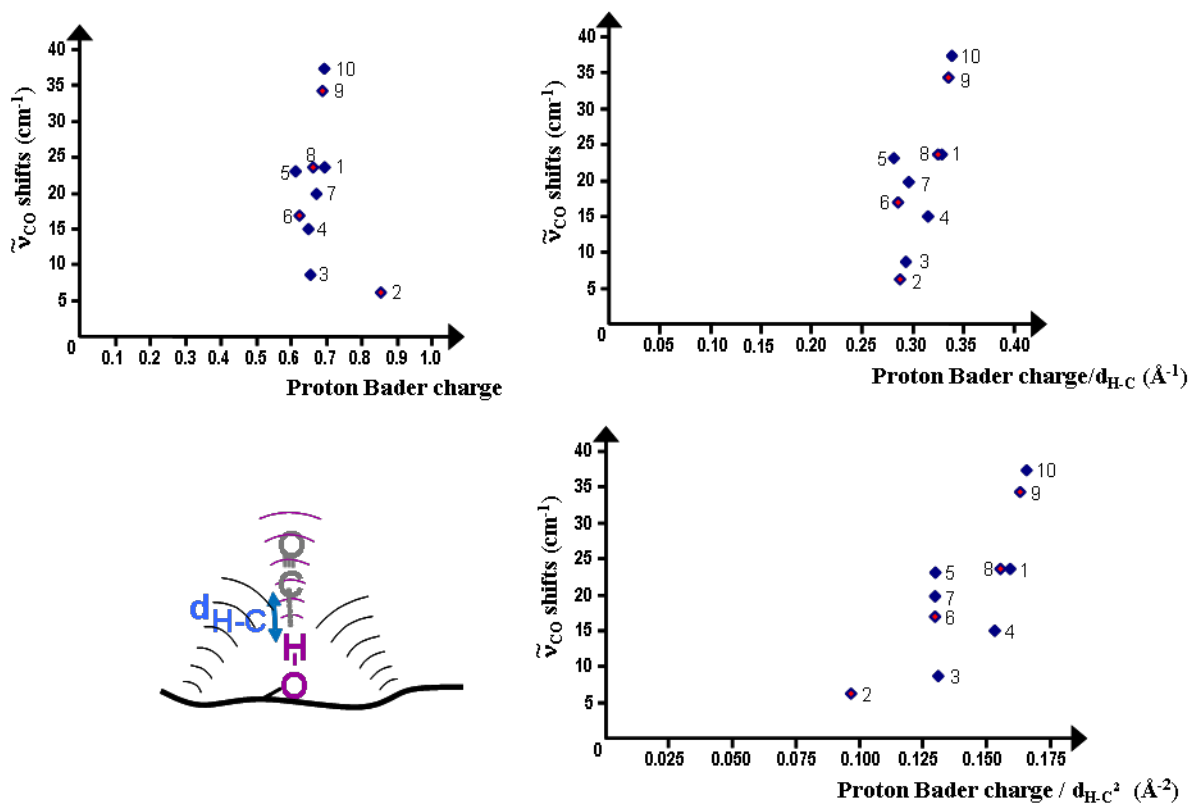


Fig. S2. $\Delta\nu_{\text{CO}}$ as function of the proton Bader charge (a), of the proton Bader charge divided by the OH-CO distance (b), and of the proton Bader charge divided by the squared OH-CO distance (c). No straight linear correlation is observed whatsoever.

S4. Lutidine / CO graphical comparison

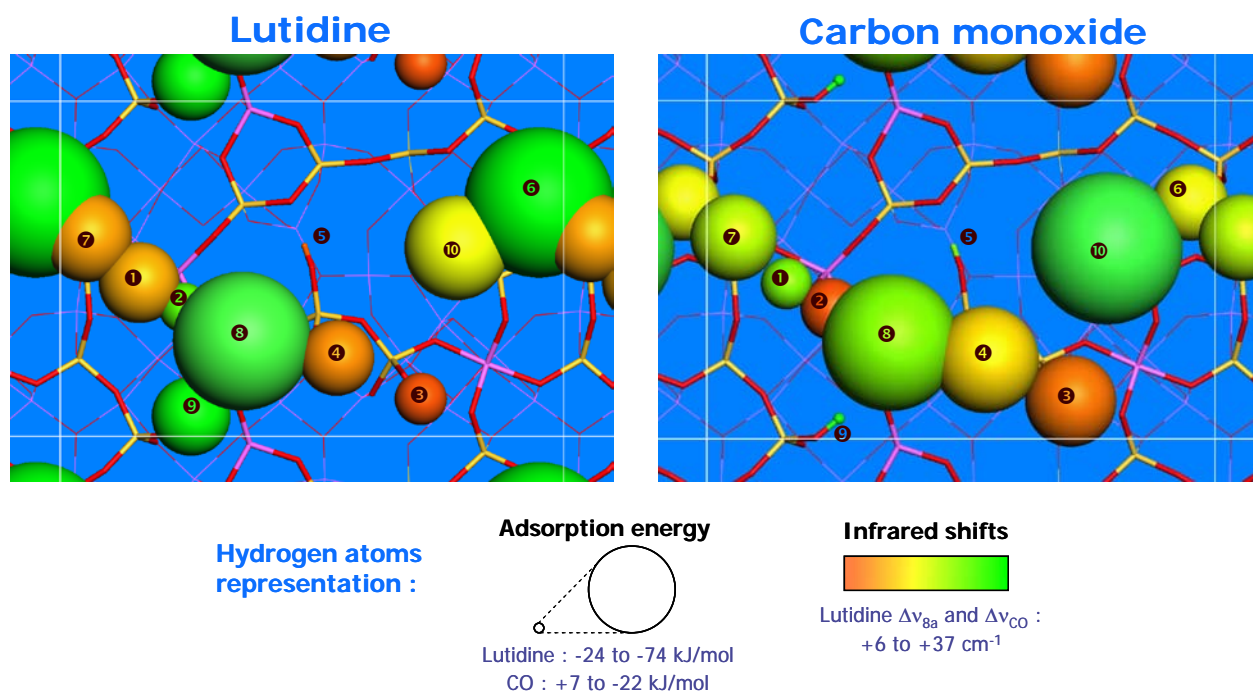


Fig. S3. Representation of the hydrogen atoms of the ASA surface model according to the adsorption energy (size) and the infrared shifts (color) of lutidine and CO. Lutidine is sensitive to the proton-donor character of the sites^[13] whereas CO is sensitive to the electrostatic field around the sites.

References

1. J. P. Perdew, Y. Wang, *Phys. Rev. B*, 1992, **45** (23), 13244-13249.
2. G. Kresse, D. Joubert, *Phys. Rev. B*, 1999, **59** (3), 1758-1775.
3. G. Kresse, J. Hafner, *Phys. Rev. B*, 1994, **49** (20), 14251-14269.
4. G. Kresse, J. Furthmüller, *Computational Materials Science*, 1996, **6** (1), 15-50.
5. G. Henkelman, A. Arnaldsson, H. Jonsson, *Computational Materials Science*, 2006, **36** (3), 354-360.
6. E. Sanville, S. D. Kenny, R. Smith, G. Henkelman, *J. Comput. Chem.*, 2007, **28** (5), 899-908.
7. K. Momma, F. Izumi, *J. Appl. Crystallogr.*, 2008, **41** (3), 653-658.
8. C. Chizallet, P. Raybaud, *Angew. Chem., Int. Ed.*, 2009, **48**, 2891-2893.
9. C. Chizallet, P. Raybaud, *ChemPhysChem*, 2010, **11** (1), 105-108.
10. M. Digne, P. Sautet, P. Raybaud, P. Euzen, H. Toulhoat, *J. Catal.*, 2002, **211**, 1-5.
11. M. Digne, P. Sautet, P. Raybaud, P. Euzen, H. Toulhoat, *J. Catal.*, 2004, **226**, 54-68.
12. F. Tielens, C. Gervais, J. F. Lambert, F. Mauri, D. Costa, *Chem. Mater.*, 2008, **20**, 3336-3344.
13. F. Leydier, C. Chizallet, A. Chaumonnot, M. Digne, E. Soyer, A. A. Quoineaud, D. Costa, P. Raybaud, *J. Catal.*, 2011, **284** (2), 215-229.
14. G. Crépeau, V. Montouillout, A. Vimont, L. Marley, T. Cseri, F. Maugé, *J. Phys. Chem. B*, 2006, **110**, 15172-15185.
15. T. P. Beebe, P. Gelin, J. T. Yates, *Surf. Sci.*, 1984, **148**, 526.
16. J. N. Kondo, R. Nishitani, E. Yoda, T. Yokoi, T. Tatsumi, K. Domen, *Phys. Chem. Chem. Phys.*, 2010, **12** (37), 11576-11586.
17. N. Nesterenko, F. Thibault-Starzyk, V. Montouillout, V. Yushchenko, C. Fernandez, J. P. Gilson, F. Fajula, I. Ivanova, *Kinetics and Catalysis*, 2006, **47** (1), 40-48.